Acute Social Stress Engages Synergistic Activity of Stress Mediators in the VTA to Promote Pavlovian Reward Learning

Jorge Tovar-Diaz[1,2], Matthew B. Pomrenze[2,3], Bahram Pahlavan[1,2], Russell Kan[4], Michael R. Drew[1,5], and Hitoshi Morikawa[1,2,*]

[1]Department of Neuroscience

[2]Waggoner Center for Alcohol and Addiction Research

[3]Division of Pharmacology and Toxicology

[4]Department of Biomedical Engineering

[5]Center for Learning and Memory

University of Texas at Austin, Austin, Texas 78712, USA

*Correspondence: morikawa@utexas.edu

ABSTRACT

Stressful events rapidly trigger activity-dependent synaptic plasticity in certain brain areas, driving the formation of aversive memories. However, it remains unclear how stressful experience affects plasticity mechanisms to regulate learning of appetitive events, such as intake of addictive drugs or palatable foods. Using rats, we show that two acute stress mediators, corticotropin-releasing factor (CRF) and norepinephrine (NE), enhance plasticity of NMDA receptor-mediated glutamatergic transmission in the ventral tegmental area (VTA) through their differential effects on inositol 1,4,5-triphosphate (IP_3)-dependent Ca^{2+} signaling. In line with this, acute social defeat stress engages convergent CRF and NE signaling in the VTA to enhance learning of cocaine-paired cues. Furthermore, defeat stress enables learning of a food-paired cue with no delay between the cue onset and food delivery. We propose that acute stress mediators synergistically regulate IP_3-Ca^{2+} signaling in the VTA to promote appetitive Pavlovian conditioning, likely enabling learning of cues with no predictive value.

INTRODUCTION

Stressor intensity, controllability, and duration are major determinants for regulation of future stress coping behavior and diverse cognitive functions (Koolhaas et al., 2011). In general, acute mild-to-moderate stress energizes adaptive cognitive processes and behaviors in the short run while severe/uncontrollable/chronic stress leads to maladaptive changes in brain function, including hippocampus-dependent learning and memory and other higher order cognitive processes (Chattarji et al., 2015; Kim et al., 2015; McEwen, 2007). As these cognitive functions are primarily declarative and studied outside the context of emotional valence, less is known about the impact of stress on reward-driven learning and behavior [see (Rodrigues et al., 2009) for stress effect on fear learning]. In this regard, stress is a well-known risk factor for the development of addiction, which can be viewed as a maladaptive form of reward learning (Sinha, 2008). While many studies have linked stress to addiction through long-term influence of glucocorticoids in the brain, stress can also exert rapid effects through the release of corticotropin-releasing factor (CRF) and norepinephrine (NE) (Joels et al., 2011; Maras and Baram, 2012). Immediate impact of stress has been studied extensively in intensification and/or reinstatement of drug seeking (Mantsch et al., 2016; Polter and Kauer, 2014); however it is not clear how stressful experience acutely regulates the acquisition of addictive behavior.

Dopamine (DA) neurons in the ventral tegmental area (VTA) play a key role in reward learning (Schultz, 2015). These neurons display transient burst firing in response to primary rewards (e.g., palatable food), while addictive drugs induce repetitive DA neuron bursting via pharmacological actions (Covey et al., 2014; Keiflin and Janak,

2015). During cue-reward conditioning, DA neurons "learn" to respond to reward-predicting cues, thereby encoding the positive emotional/motivational valence of those cues (Cohen et al., 2012; Schultz, 1998; Stauffer et al., 2016). Glutamatergic inputs onto DA neurons drive burst firing via activation of NMDA receptors (Overton and Clark, 1997; Paladini and Roeper, 2014); thus strengthening of cue-driven NMDA input may contribute to conditioned bursting. We have shown previously that repeated pairing of cue-like glutamatergic input stimulation with reward-like bursting leads to long-term potentiation (LTP) of NMDA transmission (LTP-NMDA) in DA neurons (Harnett et al., 2009). LTP induction requires amplification of burst-evoked Ca^{2+} signals by preceding activation of metabotropic glutamate receptors (mGluRs) coupled to the generation of inositol 1,4,5-triphosphate (IP_3). Here, IP_3 receptors (IP_3Rs) detect the coincidence of IP_3 generated by glutamatergic input activity and burst-driven Ca^{2+} entry. Mechanistically, IP_3 enhances Ca^{2+} activation of IP_3Rs, thereby promoting Ca^{2+}-induced Ca^{2+} release from intracellular stores (Taylor and Laude, 2002). In this study, we demonstrate how CRF and NE actions in the VTA regulate plasticity of NMDA transmission and the impact of acute stress on Pavlovian cue-reward learning.

RESULTS

Acute social stress enhances cocaine-associated cue learning

We first investigated how acute social defeat stress affects the learning of cocaine-associated cues using a conditioned place preference (CPP) paradigm. Rats underwent 30-min social defeat (~5 min of direct contact/defeat followed by ~25 min of protected threat), a form of uncontrollable psychosocial stress that elicits strong physiological

responses (Koolhaas et al., 2011). After a 10-min interval, these stressed rats and handled controls were conditioned with a relatively low dose of cocaine (5 mg/kg, i.p.; Figure 1A). This acute defeat stress–cocaine conditioning sequence was limited to a single session to eliminate the confounding effect reflecting persistent influence of stress on CPP acquisition and/or expression (Burke et al., 2011; Chuang et al., 2011; Kreibich et al., 2009; Smith et al., 2012; Stelly et al., 2016). We found that stressed rats developed larger preference for the cocaine-paired chamber compared to control rats (Figure 1B,C,F). Both stressed and control rats developed comparable robust CPP with an increase in cocaine dose (10 mg/kg) during conditioning (Figure 1D–F). Defeat stress failed to affect CPP when cocaine conditioning (5 mg/kg) was performed after a prolonged interval (1.5 hr; Figure 1G–J). These results show that social defeat stress acutely increases the sensitivity to cocaine conditioning.

CRF and NE differentially and synergistically promote NMDA plasticity in the VTA

Potentiation of NMDA excitation of DA neurons in the VTA may contribute to the learning of cues associated with rewards, including addictive drugs (Stelly et al., 2016; Wang et al., 2011; Whitaker et al., 2013; Zweifel et al., 2008; Zweifel et al., 2009). CRF and NE are the two major mediators of short-term stress effects in the brain (Joels et al., 2011; Maras and Baram, 2012). To gain insight into the mechanisms underlying acute defeat stress-induced enhancement of cocaine conditioning, we examined the effect of CRF and NE on NMDA plasticity using ex vivo VTA slices.

Induction of LTP-NMDA requires mGluR/IP_3-dependent facilitation of action potential (AP)-evoked Ca^{2+} signals (Harnett et al., 2009). CRF enhances IP_3-Ca^{2+}

84 signaling by activation of CRF receptor 2 (CRFR2) in DA neurons (Bernier et al., 2011;
85 Riegel and Williams, 2008; Whitaker et al., 2013), likely via protein kinase A (PKA)-
86 mediated phosphorylation causing increased IP_3R sensitivity (Wagner et al., 2008). To
87 first confirm this CRF effect, we assessed AP-evoked Ca^{2+} signals using the size of Ca^{2+}-
88 sensitive K^+ currents ($I_{K(Ca)}$) and a subthreshold concentration of IP_3 (10 μM·mW) was
89 photolytically applied into the cytosol for 100 ms immediately before evoking unclamped
90 APs (see Methods and Materials). Bath application of CRF (100 nM) significantly
91 increased the magnitude of IP_3-induced facilitation of $I_{K(Ca)}$ (Figure 2A,B).

92 Next, the effect of CRF on LTP-NMDA was tested using an induction protocol
93 consisting of subthreshold IP_3 application (100 ms) prior to simultaneous pairing of a
94 burst (5 APs at 20 Hz) with a brief train of synaptic stimulation (20 stimuli at 50 Hz), the
95 latter being necessary to induce LTP at specific inputs likely via activating NMDA
96 receptors at those inputs at the time of burst (Harnett et al., 2009; Stelly et al., 2016;
97 Whitaker et al., 2013). While this induction protocol using a low concentration of IP_3 (10
98 μM·mW) produced relatively small LTP in control solution, robust LTP was induced in
99 the presence of CRF (100 nM; Figure 2C–E).

100 We further examined the effect of CRF on $I_{K(Ca)}$ and LTP induction without IP_3
101 application. CRF (100–300 nM) had a small effect on $I_{K(Ca)}$ (Figure 3A,B), likely
102 reflecting facilitation of small IP_3R-mediated Ca^{2+}-induced Ca^{2+} release triggered by APs
103 themselves in DA neurons (Cui et al., 2004). Consistent with this observation, CRF failed
104 to enable measurable LTP when simultaneous synaptic stimulation-burst pairing without
105 prior IP_3 application was used to induce LTP (Figure 3C–E).

106 DA neurons express α1 adrenergic receptors (α1ARs) that are coupled to

107 phospholipase C-mediated IP_3 synthesis (Cui et al., 2004; Paladini et al., 2001).
108 Accordingly, bath application of the α1AR agonist phenylephrine (0.5–1 μM) increased
109 $I_{K(Ca)}$ in a concentration-dependent manner in the absence of exogenous IP_3 application
110 (Figure 4A,B). Phenylephrine treatment enabled robust LTP induction with simultaneous
111 synaptic stimulation-burst pairing (Figure 4C–E; see Figure 4–figure supplement 1 for
112 NE effect), in contrast to the ineffectiveness of CRF described above.

113 We next asked if CRF, via CRFR2-mediated IP_3R sensitization, could enhance
114 the effect of phenylephrine. CRF (100 nM), which had minimal effect on $I_{K(Ca)}$ by itself
115 (Figure 3A,B), significantly augmented the small $I_{K(Ca)}$ facilitation produced by a low
116 concentration (0.5 μM) of phenylephrine (Figure 5A,B), while there was no significant
117 CRF effect on $I_{K(Ca)}$ facilitation caused by 1 μM phenylephrine (Figure 5–figure
118 supplement 1). As a consequence, combined application of CRF and 0.5 μM
119 phenylephrine enabled LTP with simultaneous synaptic stimulation-burst pairing
120 protocol, comparable to LTP induced in the presence of 1 μM phenylephrine (Figure
121 5C,D).

122 Altogether, these data in VTA slices strongly suggest that CRF and NE promote
123 LTP-NMDA by differentially regulating IP_3-Ca^{2+} signaling, i.e., via CRFR2-mediated
124 increase in IP_3R sensitivity vs. α1AR-mediated generation of IP_3, enabling them to act in
125 a synergistic fashion (Figure 6A,B). LTP magnitude was positively correlated with the
126 size of $I_{K(Ca)}$ facilitation during induction across neurons with different induction
127 conditions (Figure 6C), supporting the notion that IP_3-dependent Ca^{2+} signal facilitation
128 drives LTP.
129

CRF and NE synergize in the VTA to drive stress enhancement of cocaine place conditioning

We next sought to explore if CRF and NE actions on NMDA plasticity in the VTA may contribute to social stress-induced enhancement of cocaine CPP illustrated in Figure 1. Low-dose cocaine (5 mg/kg) was used for conditioning in the following experiments to avoid the ceiling effect observed with a higher dose (Fig. 1F). Although delivery of the CRFR2 antagonist K41498 into the VTA prior to social defeat had small effect, stress-enhanced cocaine conditioning was significantly suppressed by the α1AR antagonist prazosin and abolished by co-injection of K41498 and prazosin (Figure 7A–F). Thus acute social defeat stress recruits a cooperative CRF and NE signaling mechanism acting on CRFR2 and α1AR in the VTA to promote cocaine conditioning.

Are CRF and NE actions in the VTA sufficient to enhance cocaine conditioning in the absence of stress (Figure 7G)? While control rats injected with vehicle (PBS) into the VTA developed inconsistent CPP, intra-VTA microinjection of CRF (1.5 pmol/0.3 μL/side) prior to cocaine conditioning enabled moderate CPP (Figure 7H,I,M). We further found that administration of the α1AR agonist phenylephrine (18 pmol/0.3 μL/side) lead to robust cocaine conditioning, although a lower dose (6 pmol/0.3 μL/side) had minimal effect (Figure 7J,K,M). Notably, combined application of CRF with low-dose phenylephrine enabled large CPP comparable to that observed with high-dose phenylephrine (Figure 7L,M). These data further support the idea that CRF and NE synergize in the VTA to enhance cocaine conditioning.

Acute social defeat stress promotes Pavlovian cue-food conditioning and alleviates temporal constraints on learning

LTP-NMDA in DA neurons is induced in a burst-timing-dependent manner, where the onset of glutamatergic input stimulation needs to precede postsynaptic burst, reflecting the kinetics of mGluR-induced rise in IP_3 to reach effective levels at the time of burst (Harnett et al., 2009). This timing dependence of LTP might partially account for the need of a delay between cue onset and reward delivery for the acquisition of cue-evoked DA neuron bursting (Cohen et al., 2012; Kobayashi and Schultz, 2008) and appetitive learning (Pavlov, 1927; Schwartz et al., 2002). If so, acute stress might alter the cue-reward timing rule via NE action generating IP_3, boosted by CRF effect on IP_3R sensitivity. To test this idea, we used a Pavlovian conditioned approach paradigm and varied the temporal relationship between the onset of cue (10 sec light at food magazine) and delivery of reward (food pellet) during conditioning (Figure 8A and Figure 8–figure supplement 1). While both handled controls and defeated rats developed a comparable conditioned response to the food-paired cue (magazine entry, i.e., approach to the cue light) after one conditioning session with 5 sec cue-reward delay (Figure 8B,C and Figure 8–figure supplement 2), only defeated rats developed a cue response when the cue onset and reward delivery were simultaneous (Figure 8D,E and Figure 8–figure supplement 2). Neither group developed a conditioned response when the reward was delivered 5 sec prior to cue onset (Figure 8F,G and Figure 8–figure supplement 2), suggesting that cue-encoding neural activity needs to be active at the time of reward. Thus acute defeat stress appeared to shift the cue-reward timing dependence, minimizing the requirement of delay to drive effective conditioning (Figure 8H).

DISCUSSION

Multiple stress mediators, including glucocorticoids acting via a rapid non-genomic pathway, interact, sometimes in an antagonistic fashion, to acutely regulate synaptic plasticity and learning and memory processes (Joels et al., 2011; Maras and Baram, 2012; McEwen, 2007). For example, corticosterone can promote or suppress the facilitatory effect of NE, acting via β adrenergic receptors (βARs), on synaptic plasticity depending on the timing of application in the hippocampus and amygdala (Akirav and Richter-Levin, 2002; Pu et al., 2007, 2009), while a recent study reported a synergistic action of corticosterone and CRF to impair hippocampal glutamatergic synapses and spatial memory (Chen et al., 2016). The present study demonstrates that CRF and NE synergistically augment IP_3-Ca^{2+} signaling, via CRFR2-dependent increase in IP_3 sensitivity and α1AR-dependent IP_3 synthesis, respectively, driving enhanced plasticity of NMDA transmission in VTA DA neurons. Our data further implicate a synergistic action of CRFR2 and α1AR signaling in acute social defeat stress-induced enhancement of cocaine place conditioning. Thus this study identifies a potential molecular target on which the two acute stress mediators act in concert to regulate a form of appetitive learning.

While previous studies reporting CRF/NE-induced enhancement of AMPA plasticity have mostly focused on regulation of neuronal excitability (Blank et al., 2002; Liu et al., 2017) or postsynaptic AMPA receptors (Hu et al., 2007; Seol et al., 2007), our study implicates CRF/NE effects on a Ca^{2+}-dependent induction process per se as the metaplasticity mechanism for NMDA plasticity. Interestingly, NE acting on βARs has been shown to enhance spike-timing-dependent plasticity in the hippocampus by

198 relieving the constraints on the timing of pre- and postsynaptic spikes (Lin et al., 2003;
199 Seol et al., 2007) or on the number of postsynaptic spikes (Liu et al., 2017). The current
200 study suggests that NE acting on α1ARs to generate IP_3, together with CRF facilitating
201 this α1AR effect, may remove the requirement of presynaptic stimulation preceding
202 postsynaptic bursting. Thus stress mediators appear to lower the "gate" for synaptic
203 plasticity at multiple levels in different brain areas.

204 Although our study has identified a critical role of CRFR2 in the VTA in
205 promoting NMDA plasticity and cocaine conditioning, it is known that DA neurons also
206 express CRFR1, which can control DA neuron physiology and reward/drug-driven
207 behaviors (Henckens et al., 2016). For example, while no significant effect of CRF (100–
208 300 nM) on NMDA transmission was observed in the current study, previous studies
209 have reported CRF effects on NMDA and AMPA transmission in VTA DA neurons,
210 involving multiple mechanisms via both CRFR1 and CRFR2 depending on the CRF
211 concentration used (Hahn et al., 2009; Ungless et al., 2003; Williams et al., 2014). It
212 remains to be determined how multiple CRF effects on glutamatergic transmission reflect
213 heterogeneity of DA neurons in the VTA, especially given differential effects of
214 appetitive vs. aversive/stressful stimuli on these neurons (Holly and Miczek, 2016;
215 Lammel et al., 2011; Morales and Margolis, 2017; Polter and Kauer, 2014). Regardless,
216 these CRFR1/CRFR2-dependent effects on glutamatergic excitation, together with
217 CRF/NE effects on DA neuron firing (Paladini et al., 2001; Wanat et al., 2008), may
218 contribute to the acute stress-induced enhancement of the expression of drug-seeking
219 behavior observed in vivo (Holly et al., 2016; Mantsch et al., 2016; Wang et al., 2007). It
220 should be noted that CRF and NE actions in other limbic structures also contribute to

different aspects of reward-driven behavior (Henckens et al., 2016; Otis et al., 2015; Smith and Aston-Jones, 2008). Despite the engagement of multiple brain circuits in response to acute stress-induced CRF/NE actions, our data implicate VTA DA neuron plasticity as the critical substrate for enhancement of appetitive cue learning.

The VTA receives inputs from several CRF-rich regions including the bed nucleus of the stria terminalis, central amygdala, and paraventricular hypothalamus, and paraventricular hypothalamus (Rodaros et al., 2007), while major sources of NE to the VTA are the locus coeruleus and A1, A2, and A5 noradrenergic cell groups that exhibit distinct topography of innervation to VTA subareas (Mejias-Aponte et al., 2009). Indeed, many of these brain areas are activated by social defeat stress (Martinez et al., 1998). Different types of stress may differentially recruit CRF and NE sources to the VTA, thus creating different levels of CRF and NE to regulate their synergistic interaction.

It is well known that brief stressful experience could lead to persistent changes in brain function depending on the intensity or controllability of the stressor (Musazzi et al., 2017). Indeed, a number of studies have shown persistent changes in VTA synapses lasting >1 day following single or repeated stress exposure, which are frequently linked to intensification and/or reinstatement of drug-seeking behavior (Polter and Kauer, 2014). Our previous study has shown that repeated (5 day), but not single, social defeat stress promotes the NMDA plasticity mechanism 1-10 days later, which is associated with enhanced cocaine CPP (Stelly et al., 2016). Enhancement of plasticity and CPP both require glucocorticoid action during stress exposure, likely through glucocorticoid receptors mediating long-lasting changes in gene expression. Although blockade of CRF and NE signaling in the VTA completely suppressed acute stress effect on CPP in the

current study, it may be possible that rapid non-genomic glucocorticoid effects may play a permissive role, as has been demonstrated for the effects of CRF and/or NE on synaptic function and memory processes in the hippocampus and amygdala (Chen et al., 2016; Roozendaal et al., 2008).

Interestingly, acute stress (inescapable electric shock or swim stress) has been shown to enhance Pavlovian eyeblink conditioning (Shors, 2001; Shors et al., 1992), which may be driven by a form of synaptic plasticity in the cerebellum that is dependent on an IP_3-Ca^{2+} signaling mechanism similar to NMDA plasticity in DA neurons (Wang et al., 2000). This facilitatory effect on eyeblink conditioning can be observed 30 min to 24 hr after stress exposure, while the effect on cocaine CPP was observed 30 min, but not 1.5 hr (current study) or 24 hr (Stelly et al., 2016), following a single episode of defeat stress. The role of different stress mediators underlying the persistence of single stress exposure on eyeblink conditioning has not been explored, although the effects of CRF and NE on cerebellar synaptic plasticity have been reported (Carey and Regehr, 2009; Schmolesky et al., 2007). It should also be noted that a single exposure to inescapable footshock or restraint stress has been reported to promote CPP acquisition for days (Pacchioni et al., 2002; Will et al., 1998).

In the present study, the facilitatory effect of acute social defeat stress on Pavlovian cue learning was observed not only with cocaine (i.e., drug reward) but also when food reward was used as an unconditioned stimulus (US) for conditioning. Indeed, a recent human study has reported that brief exposure to cold stress 2 min prior to Pavlovian conditioning sessions using monetary rewards promoted cue-evoked activity in the ventral striatum (Lewis et al., 2014). It is well established that the cue needs to be

267 presented prior to the US for different types of Pavlovian conditioning (Pavlov, 1927;
268 Schwartz et al., 2002). Intriguingly, stressed rats acquired a cue response (i.e., approach
269 to the cue light) even when the cue and US (food pellet) were presented simultaneously,
270 in apparent violation of a canonical principle of Pavlovian conditioning. Although
271 speculative, concerted CRF and NE actions on IP_3 signaling in VTA DA neurons might
272 mitigate the requirement of the delay from cue onset to reward delivery, during which
273 cue-evoked glutamatergic input activating mGluRs is hypothesized to cause IP_3 rise at the
274 time of reward-evoked bursting to effectively drive NMDA potentiation (Harnett et al.,
275 2009). By enabling simultaneous cue-reward conditioning, daily stressful experience may
276 lead to spurious learning of reward-associated cues with no predictive value or redundant
277 cues presented at the same time with already learned cues (e.g., money) (Holland, 1984),
278 thereby driving increased addiction liability to drug and non-drug rewards.
279

METHODS AND MATERIALS

Animals

Sprague-Dawley rats (Harlan Laboratories, Houston, Texas) were housed in pairs on a 12-hr light/dark cycle with food and water available ad libitum. All procedures were approved by the University of Texas Institutional Animal Care and Use Committee.

Brain slice electrophysiology

Midbrain slices were prepared and recordings were made in the lateral VTA located 50–150 mm from the medial border of the medial terminal nucleus of the accessory optic tract, as in our previous studies (Stelly et al., 2016; Whitaker et al., 2013). Tyrosine hydroxylase-positive neurons in this area (i.e., lateral part of the parabrachial pigmented nucleus) largely project to the ventrolateral striatum (Ikemoto, 2007) and show little VGluT2 coexpression (Trudeau et al., 2014). Internal solution contained (in mM): 115 K-methylsulfate, 20 KCl, 1.5 $MgCl_2$, 10 HEPES, 0.025 EGTA, 2 Mg-ATP, 0.2 Na_2-GTP, and 10 Na_2-phosphocreatine (pH ~7.25, ~285 mOsm/kg). Putative dopamine neurons in the lateral VTA were identified by spontaneous firing of broad APs (>1.2 ms) at 1–5 Hz in cell-attached configuration and large I_h currents (>200 pA; evoked by a 1.5 s hyperpolarizing step of 50 mV) in whole-cell configuration (Ford et al., 2006; Lammel et al., 2008; Margolis et al., 2008). Cells were voltage-clamped at –62 mV (corrected for –7 mV liquid junction potential). A 2 ms depolarizing pulse of 55 mV was used to elicit an unclamped AP. For bursts, 5 APs were evoked at 20 Hz. The time integral of the outward tail current, termed $I_{K(Ca)}$ (calculated after removing the 20 ms window following each depolarizing pulse; expressed in pC), was used as a readout of AP-evoked Ca^{2+}

303 transients, as it is eliminated by TTX and also by apamin, a blocker of Ca^{2+}-activated SK
304 channels (Cui et al., 2007).
305
306 **UV Photolysis**
307 Cells were loaded with caged IP_3 (1–10 μM) through the recording pipette. UV light (100
308 ms) was applied using the excitation light from the xenon arc lamp of the Olympus Disk
309 Spinning Unit imaging system. The light was focused through a 60× objective onto a
310 ~350 μm area surrounding the recorded neuron. Photolysis of caged compounds is
311 proportional to the UV light intensity, which was adjusted with neutral density filters and
312 measured at the focal plane of the objective (in mW). The applied IP_3 concentration is
313 expressed in μM·mW.
314
315 **LTP experiments**
316 Synaptic stimuli were delivered with a bipolar tungsten electrode placed ~200 μm rostral
317 to the recorded neuron. To isolate NMDA EPSCs, recordings were performed in DNQX
318 (10 μM), picrotoxin (100 μM), CGP54626 (50 nM), and sulpiride (100 nM) to block
319 AMPA/kainate, $GABA_A$, $GABA_B$, and D_2 dopamine receptors, and in glycine (20 μM)
320 and low Mg^{2+} (0.1 mM) to enhance NMDA receptor activation. NMDA EPSCs were
321 monitored every 20 s. The LTP induction protocol consisted of photolytic application of
322 IP_3 (10 μM·mW) for 100 ms prior to the simultaneous delivery of afferent stimulation (20
323 stimuli at 50 Hz) and postsynaptic burst (5 APs at 20 Hz), repeated 10 times every 20 s.
324 LTP magnitude was determined by comparing the average EPSC amplitude 30-40 min
325 post-induction with the average EPSC amplitude pre-induction (each from a 10 min

326 window).

327

328 **Resident-Intruder Social Defeat Paradigm**

329 Twelve week-old male resident rats were vasectomized and pair-housed with 6 week-old
330 females. Residents (used for ~8–10 months) were screened for aggression (biting or
331 pinning within 1 min) by introducing a male intruder to the home cage. Intruders and
332 controls were young males (4–5 weeks old at the beginning) housed in pairs. For defeat
333 sessions, intruders were introduced to residents' home cages after removing females.
334 Following ~5 min of direct contact, a perforated Plexiglass barrier was inserted for ~25
335 min to allow sensory contact, as in our previous study (Stelly et al., 2016). The barrier
336 was removed for a brief period (<1 min) in certain cases to encourage residents'
337 threatening behavior. Handled controls were placed in novel cages for 30 min. Intruders
338 and controls were housed separately.

339

340 **Cocaine Place Conditioning**

341 CPP boxes (Med Associates) consisting of two distinct compartments separated by a
342 small middle chamber were used for conditioning. One compartment had a mesh floor
343 with white walls, while the other had a grid floor with black walls. A discrete cue
344 (painted ceramic weight) was placed in the rear corner of each compartment (black one in
345 the white wall side, white one in the black wall side) for further differentiation. Rats were
346 first subjected to a pretest, in which they explored the entire CPP box for 15 min. The
347 percentage of time spent in each compartment was determined after excluding the time
348 spent in the middle chamber. Rats with initial side preference >60% were excluded. The

following day, rats were given a saline injection in the morning and confined to one compartment, then in the afternoon given cocaine (5 or 10 mg/kg, i.p.) and confined to the other compartment (10 min each). Compartment assignment was counterbalanced such that animals had, on average, ~50% initial preference for the cocaine-paired side. A 15 min posttest was performed 1 day after conditioning. The CPP score was determined by subtracting the preference for the cocaine-paired side during pretest from that during posttest. The experimenter performing CPP experiments was blind to animal treatments.

Intra-VTA microinjections

Rats (7–10 weeks old) were anesthetized with a mixture of ketamine and xylazine (90 mg/kg and 10 mg/kg, i.p.) and implanted with bilateral chronic guide cannulas (22 gauge; Plastics One), with dummy cannulas (32 gauge) inside, aimed at 1 mm above the VTA (anteroposterior, –5.3; mediolateral, +2.2; dorsoventral, –7.5; 10° angle). The guide cannulas were fixed to the skull with stainless steal screws and dental cement. After the surgery, rats remained singly housed for 7 days before being subjected to conditioning experiments.

Intra-VTA microinjections were made via injection cannulas (28 gauge; Plastics One) that extended 1 mm beyond the tip of the guide cannulas. Injection cannulas were connected to 1 μL Hamilton syringes mounted on a microdrive pump (Harvard apparatus). Rats received bilateral infusions (0.3 μL/side, 0.15 μL/min) of different pharmacological agents in certain conditioning experiments. The injection cannulas were left in place for 60 s after infusion.

At the end of conditioning experiments, rats were anesthetized with a mixture of

372 ketamine and xylazine (90 mg/kg and 10 mg/kg, i.p.) and transcardially perfused with 4%
373 paraformaldehyde. Brains were then carefully removed and stored in 4%
374 paraformaldehyde. Coronal sections (100 μm) were cut using a vibratome and stained
375 with cresyl violet for histological verification of injections sites (Figure 7–figure
376 supplement 1). Data from rats with injection sites outside the VTA were excluded from
377 the analysis.
378
379 **Pavlovian Conditioned Approach**
380 Conditioning was performed in modular test chambers (Med Associates) equipped with a
381 food pellet receptacle at the center of one wall. Illuminating light at the rear of receptacle
382 was used as a cue during conditioning (house light was turned off). Head entry was
383 detected with infrared photobeam positioned across the receptacle. All sessions were
384 performed on a 60 sec variable inter-trial interval schedule (range 40–80 sec). Each
385 session was preceded by a 5 min acclimation period during which rats stayed in the
386 chamber with no food pellet delivery or cue light illumination. Rats first underwent 4–7
387 days of magazine training sessions in which rats received 30 banana-flavored food pellets
388 (45 mg; Bio-Serv) with no light illumination at the receptacle and learn to rapidly (within
389 ~1 sec) respond to the food drop sound (Figure 8–figure supplement 3). To minimize
390 unconditioned response to the receptacle light, rats received 4–7 days of habituation
391 sessions where rats were exposed to 10 sec illumination of receptacle light with no food
392 delivery (15–30 trials per day; alternated with several days of magazine training
393 sessions). The final habituation session (15 trials) was used as a pretest to assess the
394 response to the cue light before conditioning. On the day following this pretest, rats

395 underwent 30 trial conditioning sessions, in which the food pellet was delivered either at
396 the onset of the 10 sec light cue, 5 sec after the cue onset (i.e., at the middle of 10 sec
397 light cue), or 5 sec before the cue onset. Posttest (15 trials, cue light with no food) was
398 performed 1 day after conditioning. Responses were measured with the proportion of
399 trials in which head entry was detected in each second (labeled P(head in)/sec). The mean
400 value during the 10 sec baseline period before cue onset was subtracted in each rat to
401 assess the cue light response. Rats displaying significant non-habituated cue response
402 during the pretest (mean P(head in)/sec >0.1 above baseline level during the 20 sec
403 period from cue onset, averaged over 15 trials) were excluded from analysis. The
404 conditioning score was determined by subtracting the mean P(head in)/sec above baseline
405 level in the pretest from that in the posttest (expressed in %).
406

407 **Drugs**

408 DNQX, picrotoxin, CGP55845, sulpiride, CRF and K41498 were obtained from Tocris
409 Biosciences. Caged IP_3 was a generous gift from Dr. Kamran Khodakhah (Albert
410 Einstein College of Medicine). All other chemicals were from Sigma-RBI.
411

412
413 **Data Analysis**

414 Data are expressed as mean ± SEM. Statistical significance was determined by Student's t
415 test or ANOVA followed by Bonferroni or Dunnett's post hoc test. The difference was
416 considered significant at $p < 0.05$.
417

418 **ACKNOWLEDGEMENTS**

419 We thank Dr. Kamran Khodakhah for the generous gift of caged IP_3 made in his lab at
420 Albert Einstein College of Medicine. We also thank Dr. Claire Stelly for comments on
421 this manuscript.

422

423 **COMPETING INTERESTS**

424 All authors declare no biomedical financial interests or potential conflict of interest.

425

426 **REFERENCES**

427

428 Akirav, I., and Richter-Levin, G. (2002). Mechanisms of amygdala modulation of
429 hippocampal plasticity. J Neurosci 22, 9912-9921.

430 Bernier, B.E., Whitaker, L.R., and Morikawa, H. (2011). Previous ethanol experience
431 enhances synaptic plasticity of NMDA receptors in the ventral tegmental area. J Neurosci
432 31, 5205-5212.

433 Blank, T., Nijholt, I., Eckart, K., and Spiess, J. (2002). Priming of long-term potentiation
434 in mouse hippocampus by corticotropin-releasing factor and acute stress: implications for
435 hippocampus-dependent learning. J Neurosci 22, 3788-3794.

436 Burke, A.R., Watt, M.J., and Forster, G.L. (2011). Adolescent social defeat increases
437 adult amphetamine conditioned place preference and alters D2 dopamine receptor
438 expression. Neuroscience 197, 269-279.

439 Carey, M.R., and Regehr, W.G. (2009). Noradrenergic control of associative synaptic
440 plasticity by selective modulation of instructive signals. Neuron 62, 112-122.

441 Chattarji, S., Tomar, A., Suvrathan, A., Ghosh, S., and Rahman, M.M. (2015).
442 Neighborhood matters: divergent patterns of stress-induced plasticity across the brain.
443 Nat Neurosci 18, 1364-1375.

444 Chen, Y., Molet, J., Lauterborn, J.C., Trieu, B.H., Bolton, J.L., Patterson, K.P., Gall,
445 C.M., Lynch, G., and Baram, T.Z. (2016). Converging, Synergistic Actions of Multiple

446 Stress Hormones Mediate Enduring Memory Impairments after Acute Simultaneous
447 Stresses. J Neurosci 36, 11295-11307.

448 Chuang, J.C., Perello, M., Sakata, I., Osborne-Lawrence, S., Savitt, J.M., Lutter, M., and
449 Zigman, J.M. (2011). Ghrelin mediates stress-induced food-reward behavior in mice. The
450 Journal of clinical investigation 121, 2684-2692.

451 Cohen, J.Y., Haesler, S., Vong, L., Lowell, B.B., and Uchida, N. (2012). Neuron-type-
452 specific signals for reward and punishment in the ventral tegmental area. Nature 482, 85-
453 88.

454 Covey, D.P., Roitman, M.F., and Garris, P.A. (2014). Illicit dopamine transients:
455 reconciling actions of abused drugs. Trends Neurosci 37, 200-210.

456 Cui, G., Bernier, B.E., Harnett, M.T., and Morikawa, H. (2007). Differential regulation of
457 action potential- and metabotropic glutamate receptor-induced Ca2+ signals by inositol
458 1,4,5-trisphosphate in dopaminergic neurons. J Neurosci 27, 4776-4785.

459 Cui, G., Okamoto, T., and Morikawa, H. (2004). Spontaneous opening of T-type Ca2+
460 channels contributes to the irregular firing of dopamine neurons in neonatal rats. J
461 Neurosci 24, 11079-11087.

462 Ford, C.P., Mark, G.P., and Williams, J.T. (2006). Properties and opioid inhibition of
463 mesolimbic dopamine neurons vary according to target location. J Neurosci 26, 2788-
464 2797.

Hahn, J., Hopf, F.W., and Bonci, A. (2009). Chronic cocaine enhances corticotropin-releasing factor-dependent potentiation of excitatory transmission in ventral tegmental area dopamine neurons. J Neurosci 29, 6535-6544.

Harnett, M.T., Bernier, B.E., Ahn, K.C., and Morikawa, H. (2009). Burst-timing-dependent plasticity of NMDA receptor-mediated transmission in midbrain dopamine neurons. Neuron 62, 826-838.

Henckens, M.J., Deussing, J.M., and Chen, A. (2016). Region-specific roles of the corticotropin-releasing factor-urocortin system in stress. Nat Rev Neurosci 17, 636-651.

Holland, P.C. (1984). Unblocking in Pavlovian appetitive conditioning. Journal of experimental psychology Animal behavior processes 10, 476-497.

Holly, E.N., Boyson, C.O., Montagud-Romero, S., Stein, D.J., Gobrogge, K.L., DeBold, J.F., and Miczek, K.A. (2016). Episodic Social Stress-Escalated Cocaine Self-Administration: Role of Phasic and Tonic Corticotropin Releasing Factor in the Anterior and Posterior Ventral Tegmental Area. J Neurosci 36, 4093-4105.

Holly, E.N., and Miczek, K.A. (2016). Ventral tegmental area dopamine revisited: effects of acute and repeated stress. Psychopharmacology (Berl) 233, 163-186.

Hu, H., Real, E., Takamiya, K., Kang, M.G., Ledoux, J., Huganir, R.L., and Malinow, R. (2007). Emotion enhances learning via norepinephrine regulation of AMPA-receptor trafficking. Cell 131, 160-173.

484 Ikemoto, S. (2007). Dopamine reward circuitry: two projection systems from the ventral
485 midbrain to the nucleus accumbens-olfactory tubercle complex. Brain Res Rev 56, 27-78.

486 Joels, M., Fernandez, G., and Roozendaal, B. (2011). Stress and emotional memory: a
487 matter of timing. Trends in cognitive sciences 15, 280-288.

488 Keiflin, R., and Janak, P.H. (2015). Dopamine Prediction Errors in Reward Learning and
489 Addiction: From Theory to Neural Circuitry. Neuron 88, 247-263.

490 Kim, E.J., Pellman, B., and Kim, J.J. (2015). Stress effects on the hippocampus: a critical
491 review. Learn Mem 22, 411-416.

492 Kobayashi, S., and Schultz, W. (2008). Influence of reward delays on responses of
493 dopamine neurons. J Neurosci 28, 7837-7846.

494 Koolhaas, J.M., Bartolomucci, A., Buwalda, B., de Boer, S.F., Flugge, G., Korte, S.M.,
495 Meerlo, P., Murison, R., Olivier, B., Palanza, P.*, et al.* (2011). Stress revisited: a critical
496 evaluation of the stress concept. Neurosci Biobehav Rev 35, 1291-1301.

497 Kreibich, A.S., Briand, L., Cleck, J.N., Ecke, L., Rice, K.C., and Blendy, J.A. (2009).
498 Stress-induced potentiation of cocaine reward: a role for CRF R1 and CREB.
499 Neuropsychopharmacology 34, 2609-2617.

500 Lammel, S., Hetzel, A., Hackel, O., Jones, I., Liss, B., and Roeper, J. (2008). Unique
501 properties of mesoprefrontal neurons within a dual mesocorticolimbic dopamine system.
502 Neuron 57, 760-773.

503 Lammel, S., Ion, D.I., Roeper, J., and Malenka, R.C. (2011). Projection-specific
504 modulation of dopamine neuron synapses by aversive and rewarding stimuli. Neuron 70,
505 855-862.

506 Lewis, A.H., Porcelli, A.J., and Delgado, M.R. (2014). The effects of acute stress
507 exposure on striatal activity during Pavlovian conditioning with monetary gains and
508 losses. Front Behav Neurosci 8, 179.

509 Lin, Y.W., Min, M.Y., Chiu, T.H., and Yang, H.W. (2003). Enhancement of associative
510 long-term potentiation by activation of beta-adrenergic receptors at CA1 synapses in rat
511 hippocampal slices. J Neurosci 23, 4173-4181.

512 Liu, Y., Cui, L., Schwarz, M.K., Dong, Y., and Schluter, O.M. (2017). Adrenergic Gate
513 Release for Spike Timing-Dependent Synaptic Potentiation. Neuron 93, 394-408.

514 Mantsch, J.R., Baker, D.A., Funk, D., Le, A.D., and Shaham, Y. (2016). Stress-Induced
515 Reinstatement of Drug Seeking: 20 Years of Progress. Neuropsychopharmacology 41,
516 335-356.

517 Maras, P.M., and Baram, T.Z. (2012). Sculpting the hippocampus from within: stress,
518 spines, and CRH. Trends in neurosciences 35, 315-324.

519 Margolis, E.B., Mitchell, J.M., Ishikawa, J., Hjelmstad, G.O., and Fields, H.L. (2008).
520 Midbrain dopamine neurons: projection target determines action potential duration and
521 dopamine D(2) receptor inhibition. J Neurosci 28, 8908-8913.

522 Martinez, M., Phillips, P.J., and Herbert, J. (1998). Adaptation in patterns of c-fos
523 expression in the brain associated with exposure to either single or repeated social stress
524 in male rats. Eur J Neurosci 10, 20-33.

525 McEwen, B.S. (2007). Physiology and Neurobiology of Stress and Adaptation: Central
526 Role of the Brain. Physiological Reviews 87, 873-904.

527 Mejias-Aponte, C.A., Drouin, C., and Aston-Jones, G. (2009). Adrenergic and
528 noradrenergic innervation of the midbrain ventral tegmental area and retrorubral field:
529 prominent inputs from medullary homeostatic centers. J Neurosci 29, 3613-3626.

530 Morales, M., and Margolis, E.B. (2017). Ventral tegmental area: cellular heterogeneity,
531 connectivity and behaviour. Nat Rev Neurosci 18, 73-85.

532 Musazzi, L., Tornese, P., Sala, N., and Popoli, M. (2017). Acute or Chronic? A Stressful
533 Question. Trends in neurosciences.

534 Otis, J.M., Werner, C.T., and Mueller, D. (2015). Noradrenergic regulation of fear and
535 drug-associated memory reconsolidation. Neuropsychopharmacology 40, 793-803.

536 Overton, P.G., and Clark, D. (1997). Burst firing in midbrain dopaminergic neurons.
537 Brain Res Brain Res Rev 25, 312-334.

538 Pacchioni, A.M., Gioino, G., Assis, A., and Cancela, L.M. (2002). A single exposure to
539 restraint stress induces behavioral and neurochemical sensitization to stimulating effects
540 of amphetamine: involvement of NMDA receptors. Ann N Y Acad Sci 965, 233-246.

541 Paladini, C.A., Fiorillo, C.D., Morikawa, H., and Williams, J.T. (2001). Amphetamine
542 selectively blocks inhibitory glutamate transmission in dopamine neurons. Nat Neurosci
543 4, 275-281.

544 Paladini, C.A., and Roeper, J. (2014). Generating bursts (and pauses) in the dopamine
545 midbrain neurons. Neuroscience 282, 109-121.

546 Pavlov, I.P. (1927). Conditioned reflexes (London, UK: Oxford University Press).

547 Polter, A.M., and Kauer, J.A. (2014). Stress and VTA synapses: implications for
548 addiction and depression. Eur J Neurosci 39, 1179-1188.

549 Pu, Z., Krugers, H.J., and Joels, M. (2007). Corticosterone time-dependently modulates
550 beta-adrenergic effects on long-term potentiation in the hippocampal dentate gyrus. Learn
551 Mem 14, 359-367.

552 Pu, Z., Krugers, H.J., and Joels, M. (2009). Beta-adrenergic facilitation of synaptic
553 plasticity in the rat basolateral amygdala in vitro is gradually reversed by corticosterone.
554 Learn Mem 16, 155-160.

555 Riegel, A.C., and Williams, J.T. (2008). CRF facilitates calcium release from
556 intracellular stores in midbrain dopamine neurons. Neuron 57, 559-570.

557 Rodaros, D., Caruana, D.A., Amir, S., and Stewart, J. (2007). Corticotropin-releasing
558 factor projections from limbic forebrain and paraventricular nucleus of the hypothalamus
559 to the region of the ventral tegmental area. Neuroscience 150, 8-13.

560 Rodrigues, S.M., LeDoux, J.E., and Sapolsky, R.M. (2009). The influence of stress
561 hormones on fear circuitry. Annu Rev Neurosci 32, 289-313.

562 Roozendaal, B., Schelling, G., and McGaugh, J.L. (2008). Corticotropin-releasing factor
563 in the basolateral amygdala enhances memory consolidation via an interaction with the
564 beta-adrenoceptor-cAMP pathway: dependence on glucocorticoid receptor activation. J
565 Neurosci 28, 6642-6651.

566 Schmolesky, M.T., De Ruiter, M.M., De Zeeuw, C.I., and Hansel, C. (2007). The
567 neuropeptide corticotropin-releasing factor regulates excitatory transmission and
568 plasticity at the climbing fibre-Purkinje cell synapse. Eur J Neurosci 25, 1460-1466.

569 Schultz, W. (1998). Predictive reward signal of dopamine neurons. J Neurophysiol 80, 1-
570 27.

571 Schultz, W. (2015). Neuronal Reward and Decision Signals: From Theories to Data.
572 Physiological reviews 95, 853-951.

573 Schwartz, B., Wasserman, E.A., and Robbins, S.J. (2002). Psychology of learning and
574 behavior, 5th edn (New York, NY: W. W. Norton & Company).

575 Seol, G.H., Ziburkus, J., Huang, S., Song, L., Kim, I.T., Takamiya, K., Huganir, R.L.,
576 Lee, H.K., and Kirkwood, A. (2007). Neuromodulators control the polarity of spike-
577 timing-dependent synaptic plasticity. Neuron 55, 919-929.

578 Shors, T.J. (2001). Acute stress rapidly and persistently enhances memory formation in
579 the male rat. Neurobiology of learning and memory 75, 10-29.

580 Shors, T.J., Weiss, C., and Thompson, R.F. (1992). Stress-induced facilitation of classical
581 conditioning. Science 257, 537-539.

582 Sinha, R. (2008). Chronic stress, drug use, and vulnerability to addiction. Ann N Y Acad
583 Sci 1141, 105-130.

584 Smith, J.S., Schindler, A.G., Martinelli, E., Gustin, R.M., Bruchas, M.R., and Chavkin,
585 C. (2012). Stress-induced activation of the dynorphin/kappa-opioid receptor system in the
586 amygdala potentiates nicotine conditioned place preference. J Neurosci 32, 1488-1495.

587 Smith, R.J., and Aston-Jones, G. (2008). Noradrenergic transmission in the extended
588 amygdala: role in increased drug-seeking and relapse during protracted drug abstinence.
589 Brain Struct Funct 213, 43-61.

590 Stauffer, W.R., Lak, A., Yang, A., Borel, M., Paulsen, O., Boyden, E.S., and Schultz, W.
591 (2016). Dopamine Neuron-Specific Optogenetic Stimulation in Rhesus Macaques. Cell
592 166, 1564-1571 e1566.

593 Stelly, C.E., Pomrenze, M.B., Cook, J.B., and Morikawa, H. (2016). Repeated social
594 defeat stress enhances glutamatergic synaptic plasticity in the VTA and cocaine place
595 conditioning. Elife 5.

596 Taylor, C.W., and Laude, A.J. (2002). IP3 receptors and their regulation by calmodulin
597 and cytosolic Ca2+. Cell Calcium 32, 321-334.

598 Trudeau, L.E., Hnasko, T.S., Wallen-Mackenzie, A., Morales, M., Rayport, S., and
599 Sulzer, D. (2014). The multilingual nature of dopamine neurons. Prog Brain Res 211,
600 141-164.

601 Ungless, M.A., Singh, V., Crowder, T.L., Yaka, R., Ron, D., and Bonci, A. (2003).
602 Corticotropin-Releasing Factor Requires CRF Binding Protein to Potentiate NMDA
603 Receptors via CRF Receptor 2 in Dopamine Neurons. Neuron 39, 401-407.

604 Wagner, L.E., 2nd, Joseph, S.K., and Yule, D.I. (2008). Regulation of single inositol
605 1,4,5-trisphosphate receptor channel activity by protein kinase A phosphorylation. J
606 Physiol 586, 3577-3596.

607 Wanat, M.J., Hopf, F.W., Stuber, G.D., Phillips, P.E., and Bonci, A. (2008).
608 Corticotropin-releasing factor increases mouse ventral tegmental area dopamine neuron
609 firing through a protein kinase C-dependent enhancement of Ih. J Physiol 586, 2157-
610 2170.

611 Wang, B., You, Z.B., Rice, K.C., and Wise, R.A. (2007). Stress-induced relapse to
612 cocaine seeking: roles for the CRF(2) receptor and CRF-binding protein in the ventral
613 tegmental area of the rat. Psychopharmacology (Berl) 193, 283-294.

614 Wang, L.P., Li, F., Wang, D., Xie, K., Wang, D., Shen, X., and Tsien, J.Z. (2011).
615 NMDA receptors in dopaminergic neurons are crucial for habit learning. Neuron 72,
616 1055-1066.

617 Wang, S.S., Denk, W., and Hausser, M. (2000). Coincidence detection in single dendritic
618 spines mediated by calcium release. Nat Neurosci 3, 1266-1273.

619 Whitaker, L.R., Degoulet, M., and Morikawa, H. (2013). Social deprivation enhances
620 VTA synaptic plasticity and drug-induced contextual learning. Neuron 77, 335-345.

621 Will, M.J., Watkins, L.R., and Maier, S.F. (1998). Uncontrollable stress potentiates
622 morphine's rewarding properties. Pharmacol Biochem Behav 60, 655-664.

623 Williams, C.L., Buchta, W.C., and Riegel, A.C. (2014). CRF-R2 and the heterosynaptic
624 regulation of VTA glutamate during reinstatement of cocaine seeking. J Neurosci 34,
625 10402-10414.

626 Zweifel, L.S., Argilli, E., Bonci, A., and Palmiter, R.D. (2008). Role of NMDA receptors
627 in dopamine neurons for plasticity and addictive behaviors. Neuron 59, 486-496.

628 Zweifel, L.S., Parker, J.G., Lobb, C.J., Rainwater, A., Wall, V.Z., Fadok, J.P., Darvas,
629 M., Kim, M.J., Mizumori, S.J., Paladini, C.A., *et al.* (2009). Disruption of NMDAR-
630 dependent burst firing by dopamine neurons provides selective assessment of phasic
631 dopamine-dependent behavior. Proc Natl Acad Sci U S A 106, 7281-7288.
632

633 **FGIRUES**

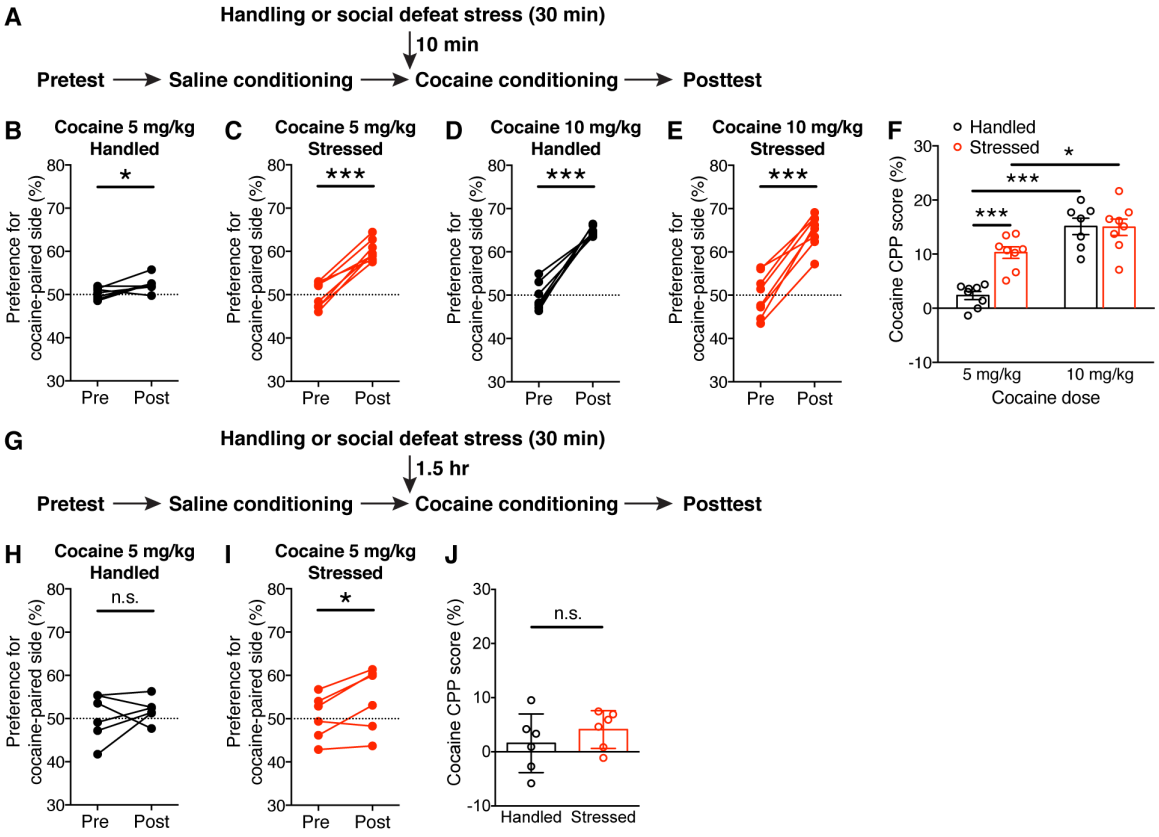

634

635 **Figure 1. Acute exposure to social defeat stress enhances cocaine place conditioning**

636 (A) Experimental timeline for testing the effect of acute social defeat stress on acquisition

637 of cocaine CPP.

638 (B–E) Changes in the preference for the cocaine-paired side in handled control rats and

639 stressed rats conditioned with 5 mg/kg or 10 mg/kg cocaine (B: $t_7 = 3.14$, $p < 0.05$; C: t_7

640 $= 9.61$, $p < 0.0001$; D: $t_6 = 9.97$, $p < 0.0001$; E: $t_7 = 9.82$, $p < 0.0001$; two-tailed paired t-

641 test).

642 (F) Summary graph demonstrating defeat stress-induced enhancement of sensitivity to

643 cocaine conditioning (stress: $F_{1,27} = 9.81$, $p < 0.01$; cocaine dose: $F_{1,27} = 49.3$, $p < 0.0001$;

644 stress × cocaine dose: $F_{1,27} = 10.62$, $p < 0.01$; two-way ANOVA). *p < 0.05, ***p <

645 0.001 (Bonferroni post hoc test).

646 (G) Experimental timeline for testing the effect of social defeat stress on cocaine CPP
647 after a 1.5-hr interval.
648 (H and I) Changes in the preference for the cocaine-paired side in rats that underwent
649 handling (H) or social defeat (I) 1.5 hr before cocaine conditioning (5 mg/kg) (H: t_5 =
650 0.71, $p = 0.51$; I: $t_5 = 2.8$, $p < 0.05$; two-tailed paired t-test).
651 (J) Graph illustrating the ineffectiveness of defeat stress on cocaine CPP with a prolonged
652 interval ($t_{10} = 0.96$, $p = 0.36$; two-tailed unpaired t-test).
653

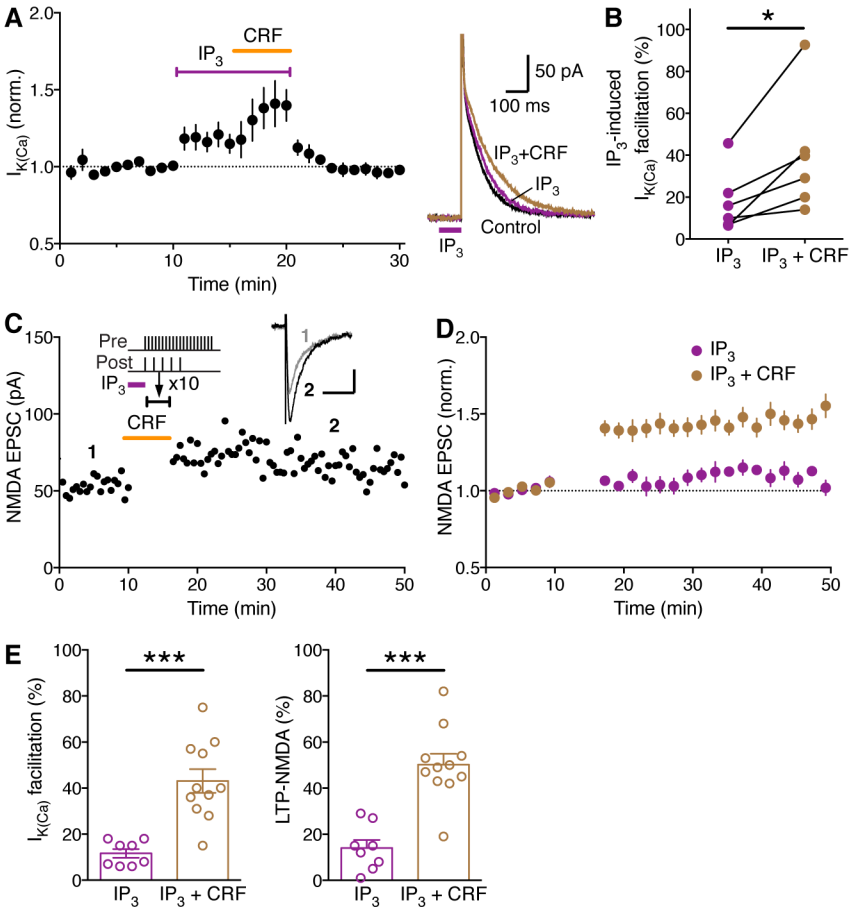

Figure 2. CRF enhances induction of LTP-NMDA driven by IP_3-induced Ca^{2+} signal facilitation in VTA dopamine neurons

(A) Summary time graph (left) and example traces (right) showing that bath application of CRF (100 nM) augments IP_3-induced facilitation of AP-evoked $I_{K(Ca)}$. Subthreshold level of IP_3 (determined as shown in Figure 2–figure supplement 1) was photolytically applied into the cytosol for 100 ms (purple bar in example traces) immediately before evoking unclamped APs (6 cells from 4 rats).

(B) Graph plotting the magnitude of IP_3-induced I_{KCa} facilitation before and after CRF application ($t_5 = 3.29$, $p < 0.05$, two-tailed paired t-test).

(C) Representative experiment to induce LTP in the presence of CRF. CRF (100 nM) was perfused for ~6 min after 10-min baseline EPSC recording, while the LTP induction

protocol, which consisted of IP_3-synaptic stimulation-burst combination (illustrated at the top), was delivered at the time indicated (10 times every 20 s; during a 3-min period starting ~3 min after the onset of CRF perfusion to allow for CRF effect to take place; see panel A). Example traces of NMDA EPSCs at times indicated are shown in inset (scale bars: 50 ms/20 pA).

(D) Summary time graph of LTP experiments in which LTP was induced using an IP_3-synaptic stimulation-burst combination protocol in control solution (8 cells from 8 rats) and in CRF (11 cells from 9 rats).

(E) Summary bar graphs depicting the magnitude of $I_{k(Ca)}$ facilitation (left) and LTP (right) for the experiments shown in (D). IP_3-induced facilitation of single AP-evoked $I_{K(Ca)}$ was assessed by comparing the size of $I_{K(Ca)}$ with and without preceding IP_3 application, which was done immediately before or after delivering the LTP induction protocol ($I_{k(Ca)}$ facilitation: $t_{17} = 5.01$, $p < 0.0001$; LTP: $t_{17} = 5.70$, $p < 0.0001$; two-tailed unpaired t-test).

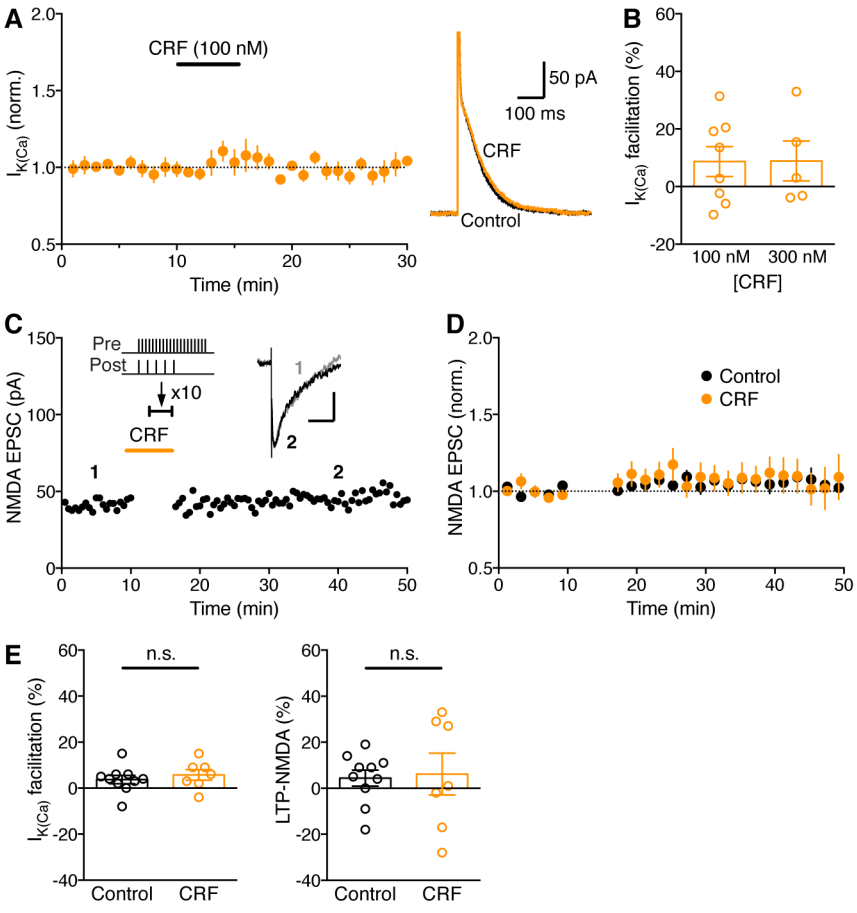

681

682 **Figure 3. CRF causes no LTP without IP_3-induced Ca^{2+} signal facilitation**

683 (A) Summary time graph (left) and example traces (right) illustrating that CRF (100 nM)

684 has small effect on $I_{K(Ca)}$ without preceding IP_3 application (8 cells from 7 rats).

685 (B) Summary bar graph showing the magnitude of $I_{K(Ca)}$ facilitation produced by two

686 concentrations of CRF (300 nM: 5 cells from 4 rats).

687 (C) Representative experiment to induce LTP in the presence of CRF using an induction

688 protocol consisting of synaptic stimulation-burst pairing with no preceding IP_3

689 application. Example EPSC traces at the times indicated are shown in inset (scale bars:

690 50 ms/20 pA).

691 (D) Summary time graph of LTP experiments in which LTP was induced using a synaptic
692 stimulation-burst pairing protocol in control solution (10 cells from 10 rats) and in CRF
693 (7 cells from 7 rats).
694 (E) Summary bar graphs depicting the magnitude of $I_{k(Ca)}$ facilitation (left) and LTP
695 (right) for the experiments shown in (D). $I_{K(Ca)}$ facilitation was assessed by comparing the
696 size of single AP-evoked $I_{K(Ca)}$ measured immediately after 10-min baseline EPSC
697 recording with that measured immediately before or after LTP induction ($I_{k(Ca)}$
698 facilitation: $t_{15} = 0.70$, $p = 0.50$; LTP: $t_{15} = 0.20$, $p = 0.84$; two-tailed unpaired t-test).
699

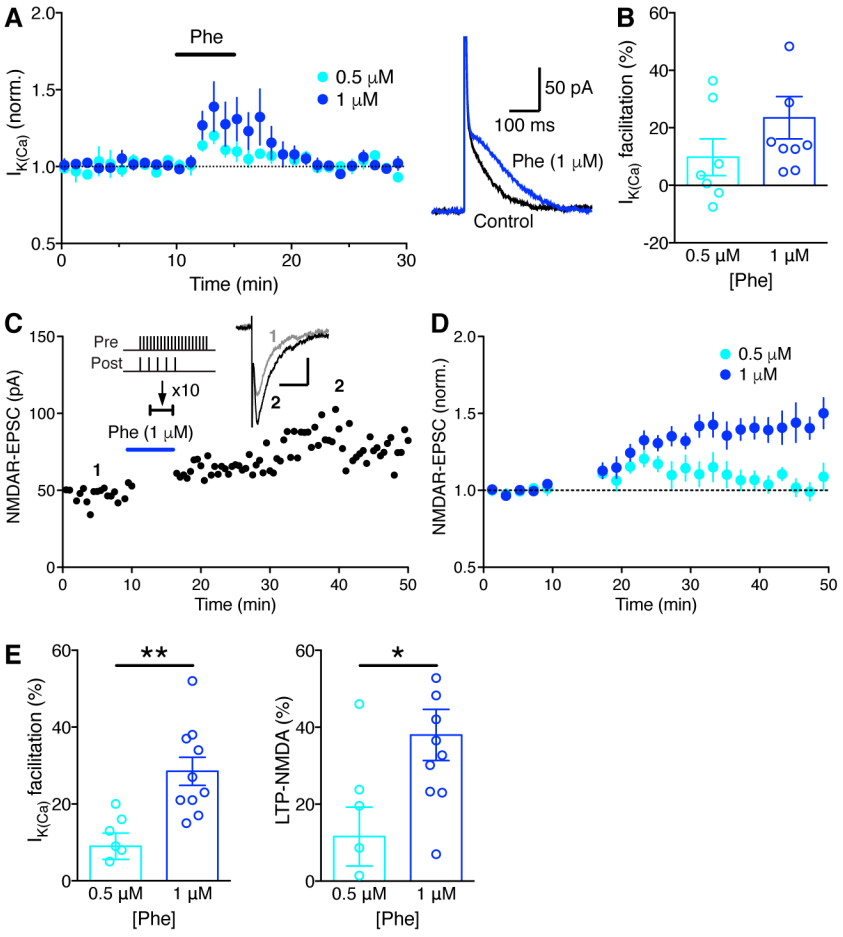

Figure 4. α1AR agonist phenylephrine enables LTP without IP_3-induced Ca^{2+} signal facilitation

(A) Summary time graph (left) and example traces (right) depicting the facilitatory effect of two concentrations of phenylephrine on $I_{K(Ca)}$ (0.5 μM: 7 cells from 3 rats; 1 μM: 9 cells from 6 rats).

(B) Summary bar graph showing the magnitude of phenylephrine-induced $I_{K(Ca)}$ facilitation.

(C) Representative experiment to induce LTP-NMDA in the presence of phenylephrine (1 μM) using an induction protocol consisting of synaptic stimulation-burst pairing with

710 no preceding IP_3 application. Example EPSC traces at the times indicated are shown in
711 inset (scale bars: 50 ms/20 pA).
712 (D) Summary time graph of LTP experiments in which LTP was induced using a synaptic
713 stimulation-burst pairing protocol in the presence of 0.5 μM or 1 μM phenylephrine (0.5
714 μM: 7 cells from 7 rats; 1 μM: 10 cells from 8 rats).
715 (E) Summary bar graphs depicting the magnitude of $I_{k(Ca)}$ facilitation (left) and LTP
716 (right) for the experiments shown in (D). $I_{K(Ca)}$ facilitation was assessed by comparing the
717 size of single AP-evoked $I_{K(Ca)}$ measured immediately after 10-min baseline EPSC
718 recording with that measured immediately before or after LTP induction ($I_{k(Ca)}$
719 facilitation: $t_{15} = 3.72$, $p < 0.01$; LTP: $t_{15} = 2.59$, $p < 0.05$; two-tailed unpaired t-test).
720
721

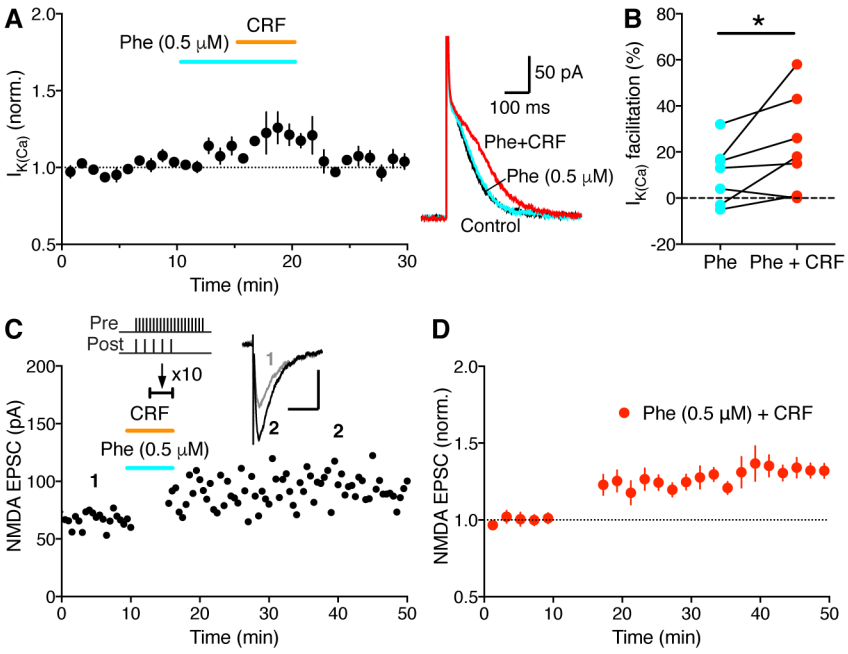

Figure 5. CRF synergizes with phenylephrine to drive LTP without IP_3-induced Ca^{2+} signal facilitation

(A) Summary time graph (left) and example traces (right) showing that CRF augments facilitation of AP-evoked $I_{K(Ca)}$ produced by a low concentration (0.5 μM) of phenylephrine (7 cells from 5 rats).

(B) Graph plotting the magnitude of I_{KCa} facilitation caused by phenylephrine (0.5 μM) alone and by CRF + phenylephrine in individual cells ($t_6 = 2.22$, $p < 0.05$, two-tailed paired t-test).

(C) Representative experiment to induce LTP in the presence of both CRF and phenylephrine (0.5 μM) using an induction protocol consisting of synaptic stimulation-burst pairing with no preceding IP_3 application. Example EPSC traces at the times indicated are shown in inset (scale bars: 50 ms/50 pA).

735 (D) Summary time graph of LTP experiments in which LTP was induced using a synaptic
736 stimulation-burst pairing protocol in the presence of both CRF and phenylephrine (0.5
737 μM) (7 cells from 4 rats).
738

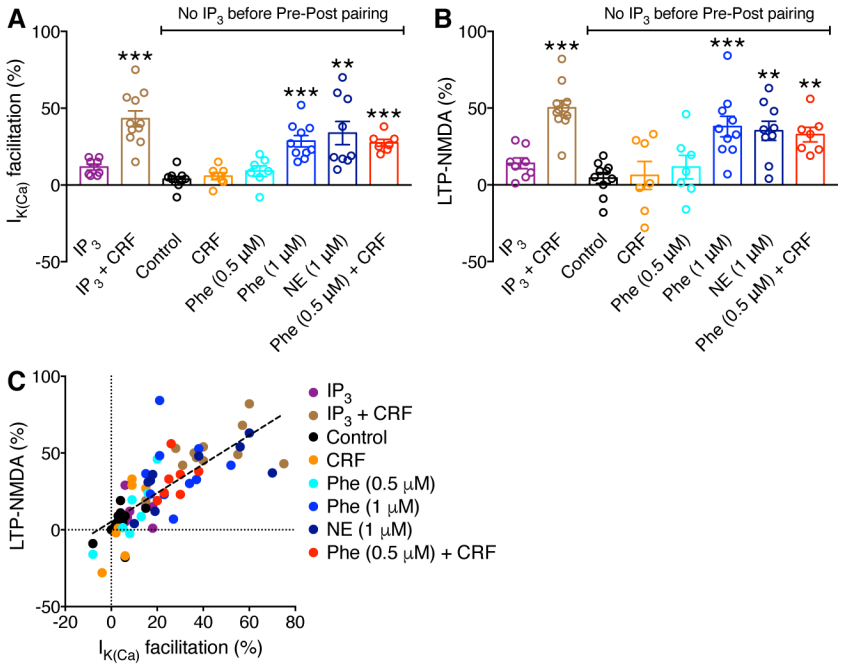

739

740 **Figure 6. Summary of LTP experiments**

741 (A and B) Summary bar graphs demonstrating the magnitude of $I_{k(Ca)}$ facilitation (A) and
742 LTP (B) for all LTP experiments testing CRF, phenylephrine, and NE (A: $F_{7,60} = 13.2$, p
743 < 0.0001; B: $F_{7,60} = 9.07$, $p < 0.0001$; one-way ANOVA). **$p < 0.01$, ***$p < 0.001$ vs.
744 control group with no IP_3 (Dunnett's post hoc test). CRF, phenylephrine, and NE had no
745 effect on NMDA transmission itself (Figure 6–figure supplement 1). (C) The magnitude
746 of LTP is plotted versus the magnitude of $I_{k(Ca)}$ facilitation in individual neurons. Dashed
747 line is a linear fit to all data points ($n = 69$, $r^2 = 0.56$).
748

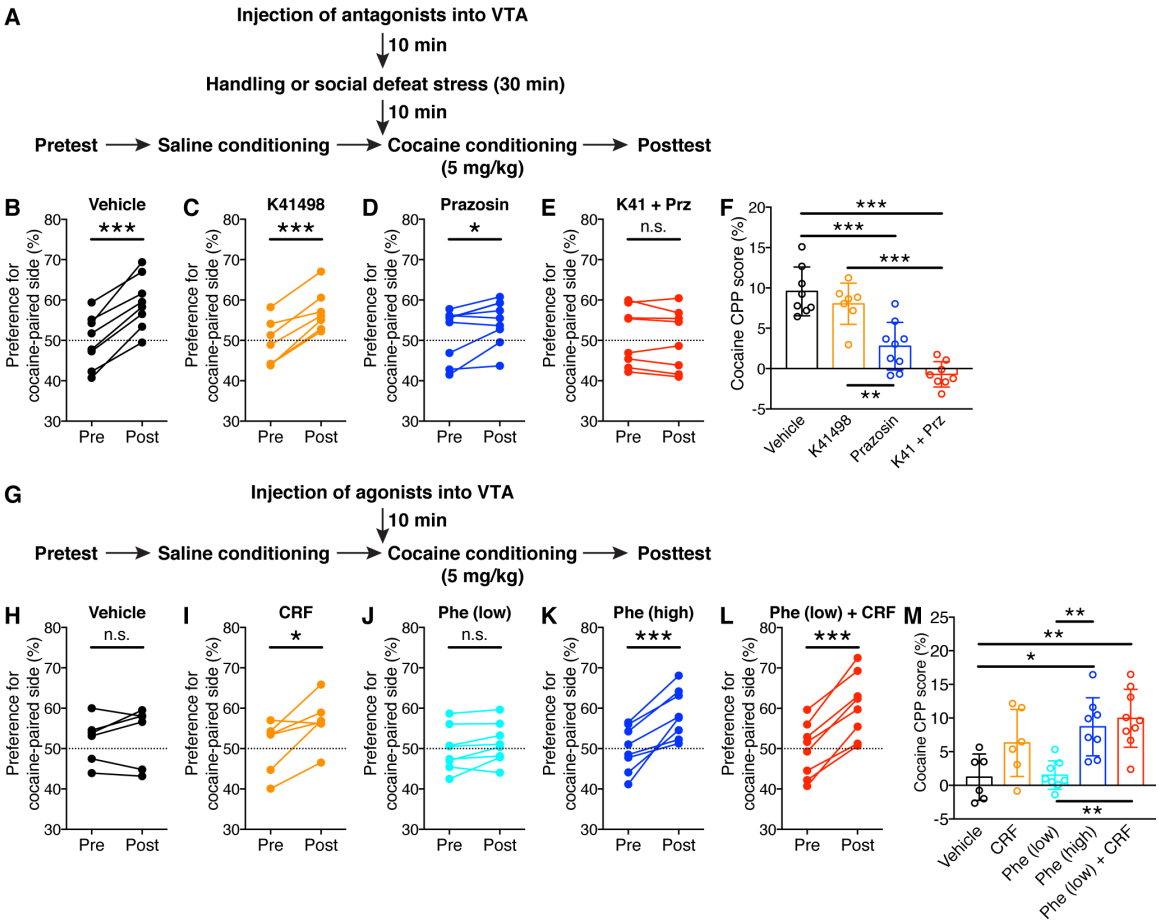

Figure 7. CRF and NE acting on CRFR2 and α1AR in the VTA synergistically promote cocaine place conditioning

(A) Experimental timeline for testing the effects of intra-VTA injection of CRFR2 antagonist K41498 and α1AR antagonist prazosin on defeat stress-induced enhancement of cocaine conditioning.

(B–E) Changes in the preference for the cocaine-paired side (conditioned with 5 mg/kg cocaine) in socially defeated rats that received intra-VTA injection of PBS (B), K41498 (C), prazosin (D), or a cocktail of K41498 and prazosin (E) (H: $t_7 = 8.97$, $p < 0.0001$; I: $t_7 = 4.03$, $p < 0.01$; J: $t_8 = 2.82$, $p < 0.05$; K: $t_7 = 1.27$, $p = 0.24$; two-tailed paired t-test).

759 (F) Summary graph demonstrating CRFR2 and α1AR dependence of stress-induced
760 enhancement of cocaine conditioning ($F_{3,30} = 14.5$, $p < 0.0001$, one-way ANOVA). **p <
761 0.01, ***p < 0.001 (Bonferroni post hoc test).
762 (G) Experimental timeline for testing the effects of intra-VTA injection of CRF and
763 phenylephrine on acquisition of cocaine CPP in non-stressed rats.
764 (H–L) Changes in the preference for the cocaine-paired side (conditioned with 5 mg/kg
765 cocaine) in rats that received intra-VTA injection of PBS (H), CRF (I), high-dose
766 phenylephrine (18 pmol/0.3 μL; J), low-dose phenylephrine (6 pmol/0.3 μL; K), or a
767 cocktail of CRF and low-dose phenylephrine (L) (B: $t_7 = 0.40$, $p = 0.70$; C: $t_7 = 2.28$, $p =$
768 0.057; D: $t_7 = 5.69$, $p < 0.001$; E: $t_7 = 2.02$, $p = 0.083$; F: $t_7 = 8.89$, $p < 0.0001$; two-tailed
769 paired t-test).
770 (M) Summary graph demonstrating the effects of CRF and phenylephrine on cocaine
771 place conditioning in the absence of stress ($F_{4,36} = 5.17$, $p < 0.01$, one-way ANOVA). *p
772 < 0.05, **p < 0.01 (Bonferroni post hoc test).
773

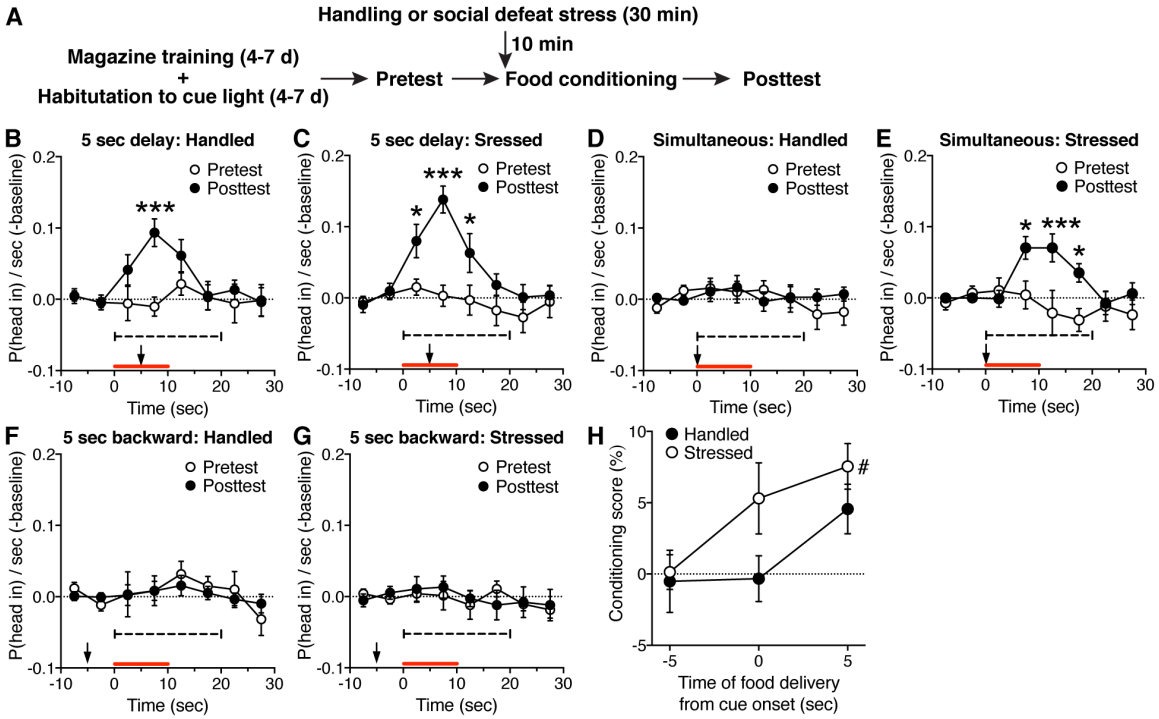

774

775 **Figure 8. Acute social defeat stress enables learning of a food-paired cue with no**

776 **delay between cue onset and food delivery.**

777 (A) Experimental timeline for testing the effect of acute social defeat stress on food

778 conditioned approach.

779 (B–G) Summary time graphs showing cue responses (binned in 5 sec) before and after

780 conditioning in handled and defeated rats (B: 9 rats, C: 11 rats, D: 12 rats, E: 11 rats, F: 9

781 rats, G: 10 rats). Cue light was presented at the red bar, while the arrow indicates the time

782 of food delivery during conditioning (B: time: $F_{7,56} = 3.30$, $p < 0.01$; time × test: $F_{7,56} =$

783 2.31, $p < 0.05$; C: time: $F_{7,70} = 7.22$, $p < 0.0001$; test: $F_{1,10} = 19.2$, $p < 0.01$; time × test:

784 $F_{7,70} = 4.81$, $p < 0.001$; E: time: $F_{7,70} = 3.34$, $p < 0.01$; time × test: $F_{7,56} = 3.30$, $p < 0.01$;

785 repeated measures two-way ANOVA). (H) Summary graph illustrating the cue-reward

786 timing dependence of conditioning in control and stressed rats (time of food: $F_{2,56} = 5.33$,

787 $p < 0.01$; stress: $F_{1,56} = 4.09$, $p < 0.05$; two-way ANOVA). Conditioning score (expressed

788 in %) was calculated from the 20 sec period at the dashed line in (B)–(G). *$p < 0.05$,

789 ***$p < 0.001$ vs. pretest in (B), (C), and (E); $^{\#}p < 0.05$ vs. -5 sec group in (H) (Bonferroni

790 post hoc test).

791

792 **FIGURE SUPPLEMENTS**

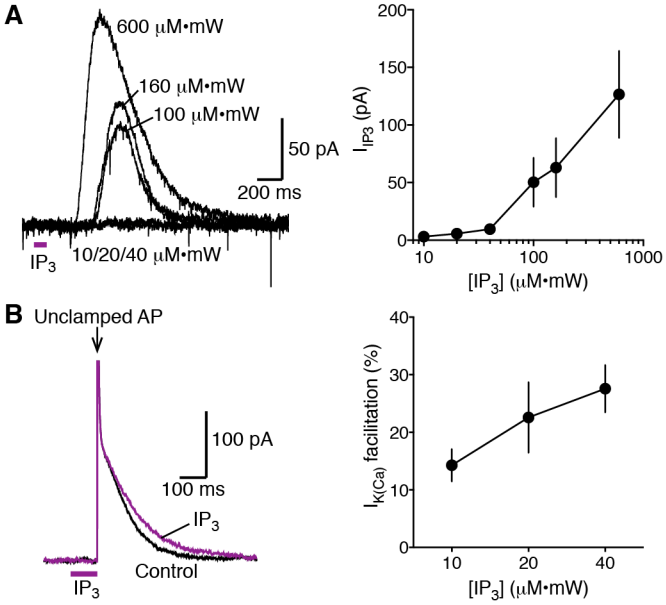

793

794 **Figure 2–figure supplement 1.**

795 (A) Example traces and summary graph depicting the concentration dependence of IP_3-
796 evoked outward currents. Data were obtained from 7 cells, where six different IP_3
797 concentrations (10, 20, 40, 100, 160, and 600 μM·mW; photolytically applied for 100
798 ms) were tested in each cell.

799 (B) Example traces (using 40 μM·mW IP_3) and summary graph illustrating facilitation of
800 AP-evoked $I_{K(Ca)}$ caused by near-threshold levels of IP_3 (10, 20, and 40 μM·mW; n = 14,
801 7, and 7, respectively). Note the relatively long latency (~200–400 ms) following IP_3
802 application to evoke response at suprathreshold range (100, 160, and 600 μM·mW),
803 which reflects the time required to engage the regenerative IP_3R-mediated Ca^{2+}-induced
804 Ca^{2+} release process. In contrast, IP_3 effect on AP-evoked $I_{K(Ca)}$ occurs with no latency, as
805 rapid Ca^{2+} influx triggered by APs initiates the Ca^{2+}-induced Ca^{2+} release process, which
806 can be augmented by near-threshold levels of IP_3.

807

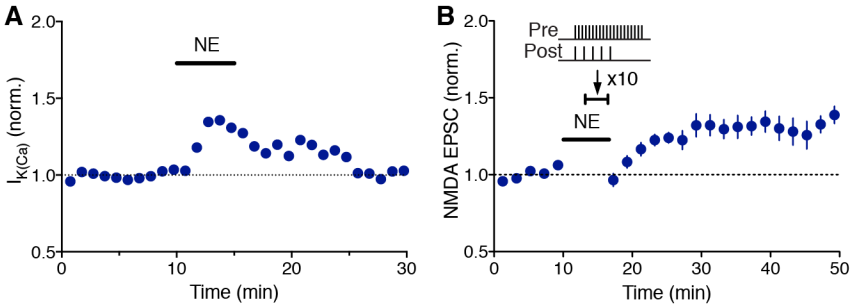

808

809 **Figure 4–figure supplement 1.**

810 (A) Summary time graph showing the facilitatory effect of NE (1 μM) on AP-evoked

811 $I_{K(Ca)}$ (n = 5).

812 (B) Summary time graph of LTP-NMDA experiments in which LTP was induced using a

813 synaptic stimulation-burst pairing protocol in the presence of NE (1 μM; n = 9).

814

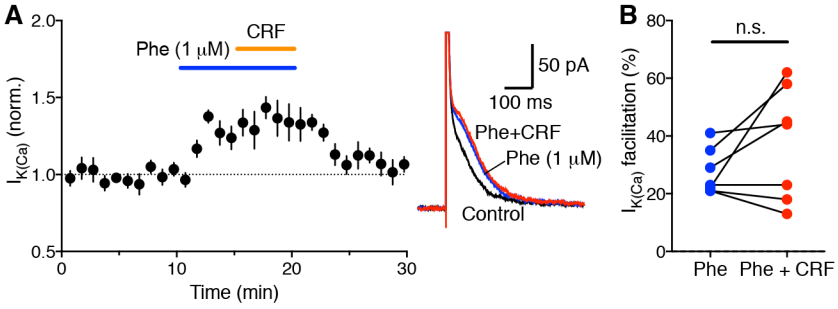

815

816 **Figure 5–figure supplement 1.**

817 (A) Summary time graph (left) and example traces (right) showing that CRF does not

818 have significant effect on AP-evoked IK(Ca) facilitated by a high concentration (1 μM)

819 of phenylephrine (n = 9).

820 (B) Graph plotting the magnitude of IK(Ca) facilitation caused by phenylephrine (1 μM)

821 alone and by CRF + phenylephrine in individual cells (t_6 = 1.57, p = 0.17, two-tailed

822 paired t-test).

823

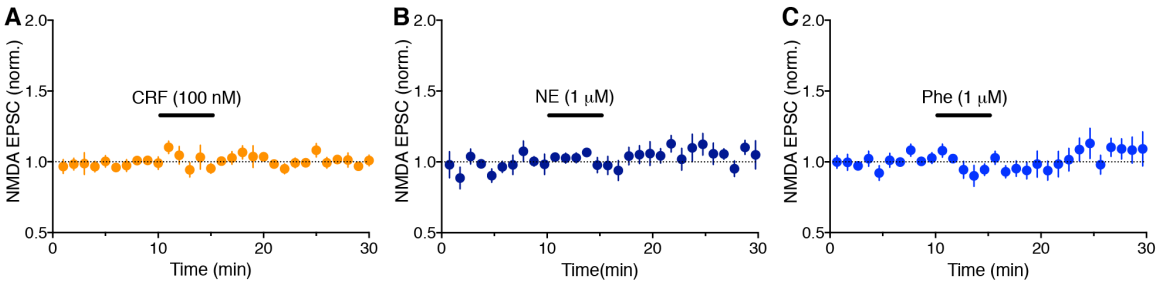

Figure 6–figure supplement 1.

Summary time graphs showing that CRF (A: n = 5), NE (B: n = 7), and phenylephrine (C: n = 5) have no measurable effect on NMDA EPSCs.

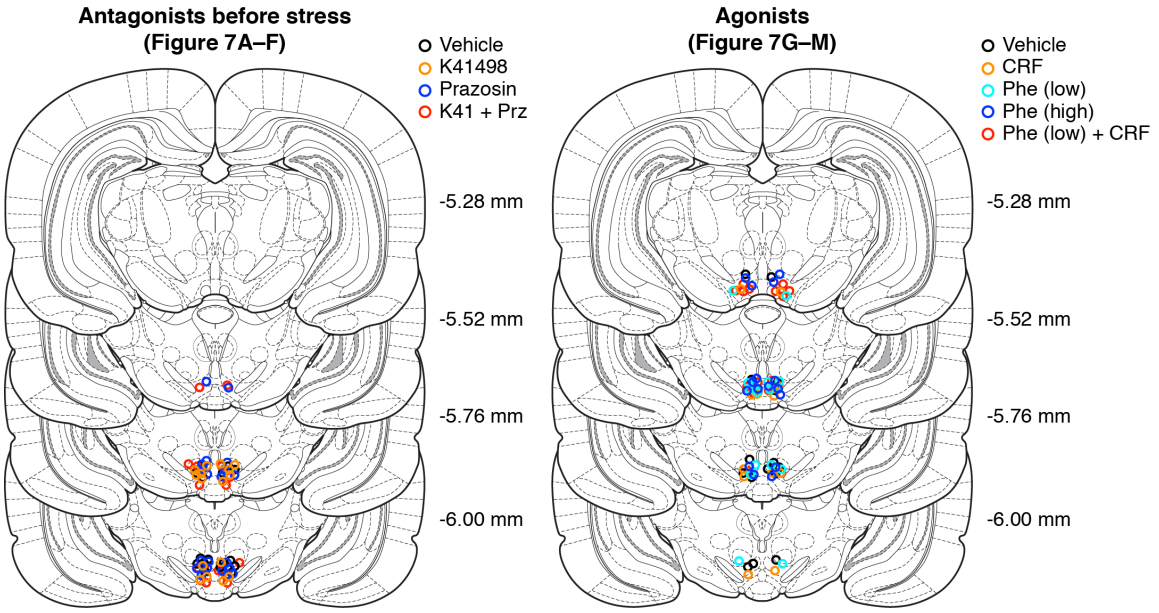

Figure 7–figure supplement 1.

Approximate locations (mm from bregma) of cannula tips for intra-VTA microinjection experiments in Figure 7.

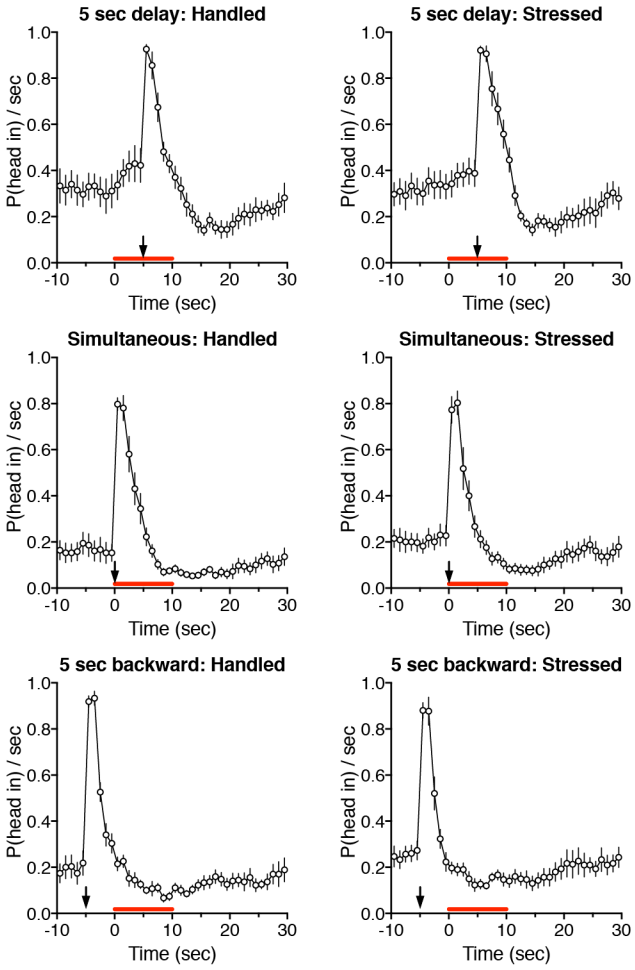

834

835 **Figure 8–figure supplement 1.**

836 Time graphs illustrating head entry responses during conditioning sessions. The 10 sec

837 cue light was presented at the red bar, while food was delivered at arrow.

838

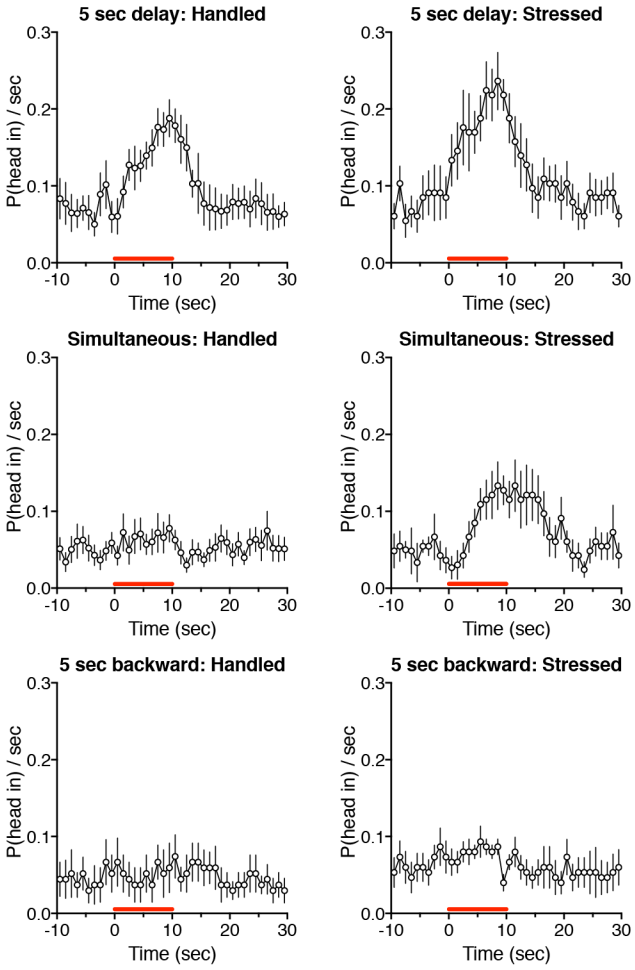

Figure 8–figure supplement 2.

Time graphs illustrating head entry responses during posttests. The 10 sec cue light was presented at the red bar.

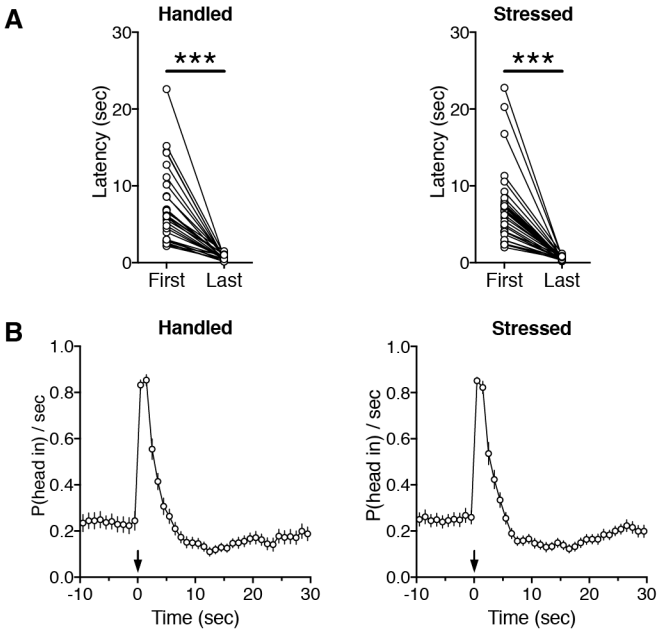

Figure 8–figure supplement 3.

Graphs depicting head entry responses during magazine training sessions before undergoing handling/social defeat and conditioning sessions.

(A) Mean latency to the first head entry after food delivery is plotted during the first and last magazine training sessions in individual rats. Data are from all rats shown in Figure 8 (handled: $t_{29} = 7.52$, $p < 0.0001$; stressed: $t_{31} = 7.53$, $p < 0.0001$; paired t-test).

(B) Time graphs plotting the probability of head entry into the food magazine during the last magazine training session. Food was delivered at arrow.